Quantification of gray/white matter in neonates and adults.

B C Lee, B Kneeland, R J Knowles and P T Cahill

AJNR Am J Neuroradiol 1983, 4 (3) 692-695
http://www.ajnr.org/content/4/3/692

Quantification of Gray/White Matter in Neonates and Adults

B. C. P. Lee,[1] B. Kneeland,[1] R. J. R. Knowles,[1] and P. T. Cahill[1,2]

Quantitation of gray/white matter is important in evaluation of cerebral blood flow, atrophy, and development of the brain. First-order statistical analysis of neonatal computed tomographic (CT) images revealed that there was only a 6 Hounsfield unit (H) difference between gray and white matter compared with the observed 3 H for the standard deviation over the field of a skull water phantom. Scene segmentation methods based on first-order statistics proved unsuccessful in separating gray and white matter. A new regional clustering algorithm based on local textural properties was developed for separation of these structures.

For the evaluation of cerebral blood flow, atrophy, and neurologic development of the neonatal brain it is of great importance to be able to quantitate gray and white matter on computed tomographic (CT) scans. In adults and older infants white matter is well myelinated and has less photoelectric absorption than gray matter [1]. In premature neonates white matter has little myelin but high water content, which accounts for lower Hounsfield numbers [2]. Although visual differences can readily be observed in gray and white matter, the quantification of the relative amounts of gray and white matter (using first-order statistical image segmentation methods) has so far proven elusive. This is due in part to small CT density differences, the complex interdigitation of gray/white matter, the inherent noise spectrum present in CT scanners, and partial volume effects. In addition, statistical variations at gray/white matter borders greatly complicate the local topography; thus scene segmentation of gray/white matter would require greater spatial resolution and signal-to-noise ratio than are currently available. In brief, the reason that visual differences in gray and white matter are observed is higher-order textural differences, not first-order statistical differences.

The purpose of this study was to develop methods of statistical analysis of CT attenuation value that use these textural differences to convert what is visualized into quantitative values of gray/white matter.

Materials and Methods

Cranial CT was performed in eight neonates (1,500 g or less) and six adults using a GE CT/T 8800. Scanning technique factors were 480–700 mAs at 120 keV. Reconstructed CT images were transferred to magnetic tape and analyzed on a Varian V76 computer with 256 kbytes memory and 9.6 Mbytes disk space. All images were processed either as the originally reconstructed 320 × 320 matrices or as zoomed 64 × 64 matrices. Displays (statistically coded images or three-dimensional relief maps) were obtained using a Statos electrostatic printer/plotter.

To investigate the sensitivity of our new texture-discrimination scene-segmentation algorithms, several phantoms were developed to test textural quantification of gray/white matter from CT scans. These included plexiglass, contrast material in water, and various mixtures of graduated pasta particles of 0.1–5 mm. A neonatal skull filled with water was used to measure instrumental noise over the range of miliamperage values clinically used. Formalin-fixed pathologic sections were photographed and digitized as well.

CT images of the phantoms and gray/white matter were analyzed for their first- and higher-order statistical properties. First-order parameters were the first, second, and third moments of local 16 × 16 matrices. For the higher-order parameters, the magnitude and direction of the local gradient, the energy, inertia, and correlation were calculated for overlapping and nonoverlapping local matrices, which varied from 2 × 2 to 4 × 4 in size. To determine the differences in both first- and second-order parameters, the changes in gray and white matter were examined on CT images where regions could be definitely called gray or white by visual inspection. Since white matter predominates over gray matter, most CT images contained several independent white-matter regions of 16 × 16 pixels (normal image, 320 × 320), while normally only one such region could be assigned to gray matter. In addition to these statistical parameters, the two-dimensional frequency spectrum was calculated using a fast-Fourier transformation and the power spectrum was displayed as two-dimensional relief maps. The autopower spectrum for each gray/white region also was calculated for the skull, water, and texture phantoms.

A regional-clustering algorithm was developed to separate gray and white matter. Because white matter predominates in CT transverse images, the regional clustering algorithm is initially started inside a white-matter region. The regional-clustering algorithm then proceeds outward, bound by two constraints: the white region must exhibit simple connectivity, and the region must conform to the smooth topology imposed by anatomic structure. Subject to these two physical constraints, a threshold determined by the local first-

[1]Department of Radiology, New York Hospital–Cornell Medical Center, 525 East 68th Street, New York, NY 10021. Address reprint requests to B. C. P. Lee.
[2]Polytechnic Institute of New York, Brooklyn, NY 11201.

AJNR 4:692–695, May/June 1983 0195-6108/83/0403-0692 $00.00

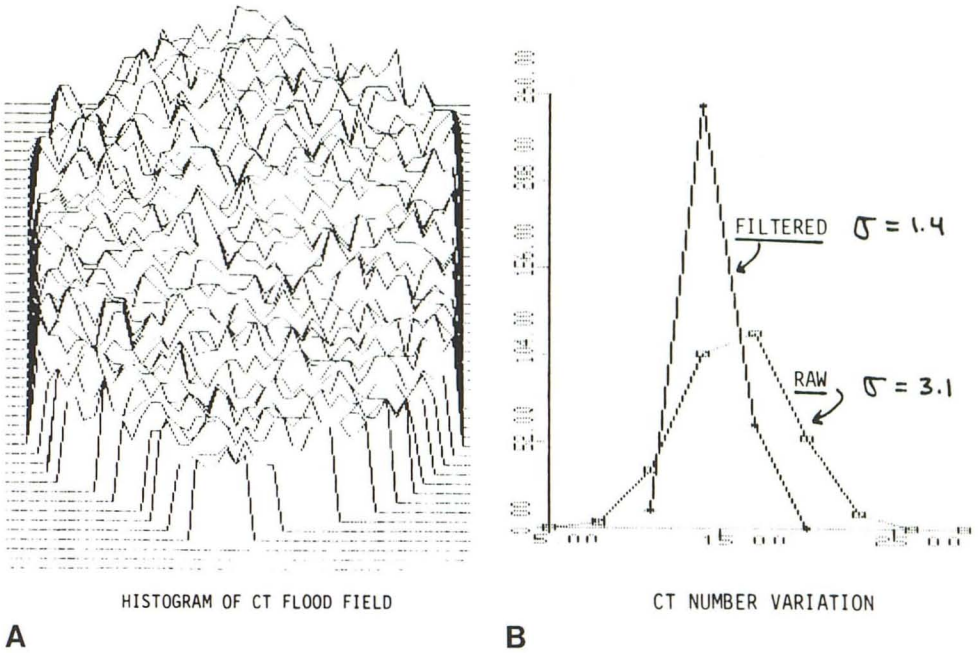

Fig. 1.—**A**, Relief map of flood field of water-filled skull phantom. Note nonuniformity of field. **B**, Graph shows variation in CT numbers (X axis) vs. total number of pixels (Y axis) of flood field before and after filtration.

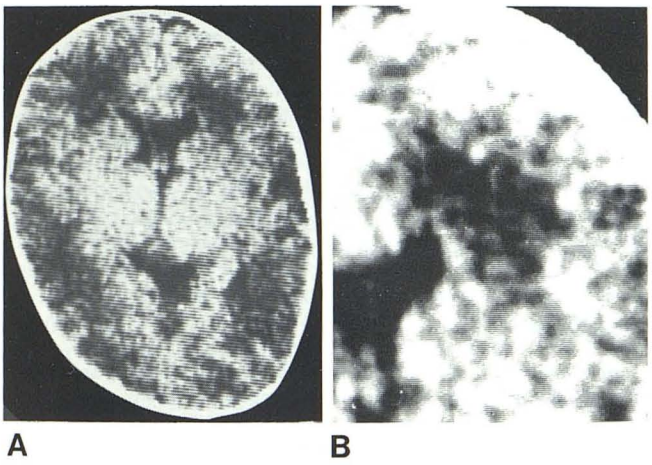

Fig. 2.—**A**, Plain CT of neonatal brain distinguishes between gray and white matter. **B**, Zoomed magnified image of right upper quadrant. Margin between gray and white matter is no longer obvious.

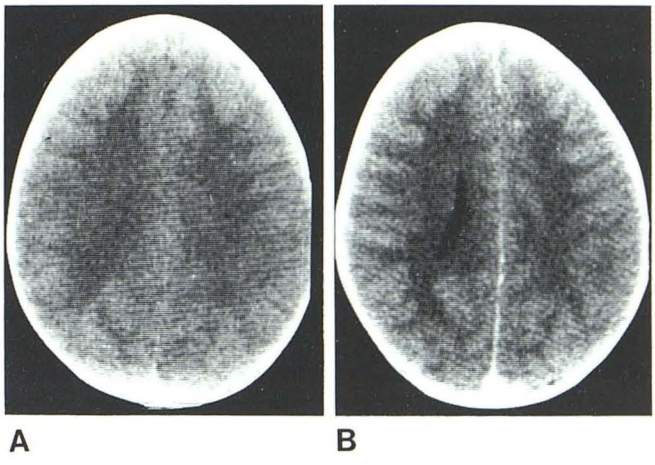

Fig. 3.—CT section of adult brain. **A**, Plain CT. Gray and white matter are distinct, but margins are indistinct. **B**, Postcontrast CT. Gray/white matter now clearer, but texture of white matter is reduced compared with **A**.

order averages of the 16 × 16 matrices can be applied to local areas of the CT image. Normally, 3 × 3 local matrices were found to be optimal, for the regional-clustering algorithm was repeated one to three times until the image stabilized. The regional-clustering algorithm considers the differences in noise spectrum or texture between the gray and white matter and operates on white regions, which are more uniform in texture [3].

To account for variations in equipment performance for different studies, each patient served as his own control. The functional parameters used in the regional clustering were determined for each study using unambiguous local regions of both white and gray matter.

Results

Spatial Resolution and Noise Spectrum of CT Scanner

The resolution and intrinsic instrumental noise spectrum was determined using a plexiglass GE water phantom [4]. Variations of about 10 Hounsfield units (H) across the field were normally observed in the water phantom with 3–5 SD. Using a pediatric skull phantom filled with water, the observed standard deviation varied from 2.8 to 3.5 H depending on the milliamperage values (fig. 1). This reduction is in part due to the shaped bow-tie filter where a better image reconstruction is achieved due to partial correction of beam hardening. When the regional-clustering algorithm was applied to the skull phantom, the standard deviation was further reduced to 1.4–1.6 H.

Gray/White Differences in CT Density

Although gross regional differences in gray and white matter can be readily discerned on CT slices with appropriate window settings, visual scene segmentation on zoomed sections by several different observers was unsuccessful because of the complex interdigitations between white and gray matter (fig. 2). Measurements in regions visually identified as gray or white showed about 6 H separating the

first moments of the white and gray zones. Since the standard deviation of the skull phantom fields was 3 H, separation depending on first-order statistics was therefore exceedingly difficult, considering the partial-volume effect of the scanner and the complex topography of gray/white matter. Studies with intravenous contrast material showed that although the white matter is distinctly enhanced visually, the average difference in Hounsfield numbers between the gray and white matter is not increased (fig. 3). There is also a reduction in the white-matter texture.

Therefore, quantitative scene segmentation based on first-order differences could not be made either with or without intravenous contrast media. On the other hand, it is a well known fact that the human visual system is sensitive to second- and third-order statistics. For these reasons, methods of image processing that use more sophisticated scene segmentation methods involving higher-order statistics are needed to quantitate the relative amounts of gray/white matter.

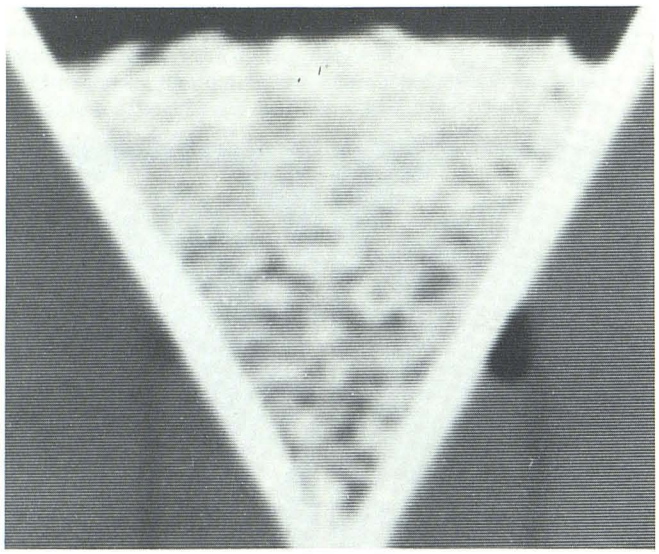

Fig. 4.—Texture phantom. Conical plexiglass cylinder contains matter of similar CT numbers but different textures.

Scene Segmentation Based on Textural Differences

A direct comparison of the CT slices with pathologic sections proved more difficult than originally expected due to scaling of the images and difficulty in matching the CT sections with the anatomic sections. The pathologic slices were digitized as 128 × 128 matrices, and matching them to the 320 × 320 CT image's anatomic landmarks proved exceedingly difficult. Again, this is because the boundaries between the gray and white matter are very complex. Currently, a 512 × 512 digitizing system is being evaluated for matching with 320 × 320 CT images. Scaling is being performed by appropriate zooming of known anatomic distances determined by the size of the ventricles and the outer border of the brain.

In order to test the ability of the regional-clustering algorithm to quantitate gray/white matter differences, cylindrical plexiglass phantoms were constructed so that the central conical defect could be filled with material that had Hounsfield numbers within 3–6 H of plexiglass, but had significantly different textural properties (fig. 4). (The conical shape permits an analysis of the effectiveness of both first-order and higher-order scene-segmentation algorithms.) Our validated nearest-neighbor edge-detection algorithm [5] was unable to separate the edges of the cone on a first-order test. The criterion for scene segmentation is the linearity of the two conical edges, which is not dependent on partial-volume effects, milliamperage values, or field uniformity, as shown in figure 5. On the other hand, our regional-clustering algorithm functioning on the differences between the texture properties of the outside plexiglass and inside conical zone could easily delimit this boundary.

In figure 6, a zoomed (64 × 64) statistical map is shown of the CT numbers of the left frontal lobe of figure 3. Each symbol differs by 3H, which is consistent with the observed standard deviation of the noise level in the skull phantom. At the statistical confidence level of 1 SD, separation of gray/white structure is not evident; however, if our regional-clustering algorithm is applied to the same data, the typical gray/white separation observed on pathologic sections is clearly demonstrated.

Discussion

Because CT number variation caused by instrumental noise is very close to the difference between gray- and white-matter readings, quantitative separation of these structures based on first-order statistics (using methods such as the nearest-neighbor edge-detection algorithms) was unsuccessful, even though it is visually possible

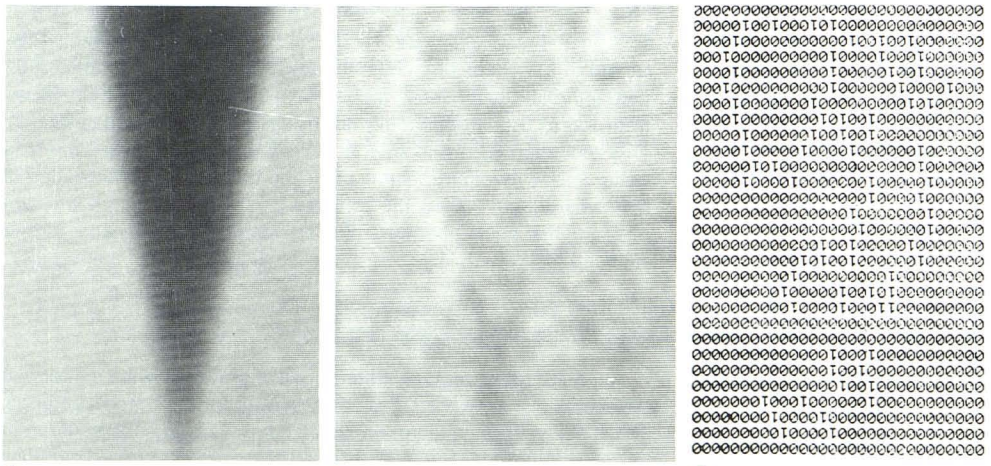

A B C

Fig. 5.—Conical plexiglass phantom filled with water **(A)** and with material of similar CT number but with texture **(B)**. It is not possible to separate contents from plexiglass wall. **C**, Nearest-neighbor edge-detection algorithm applied to texture phantom. Note lack of clear edge of vessel wall.

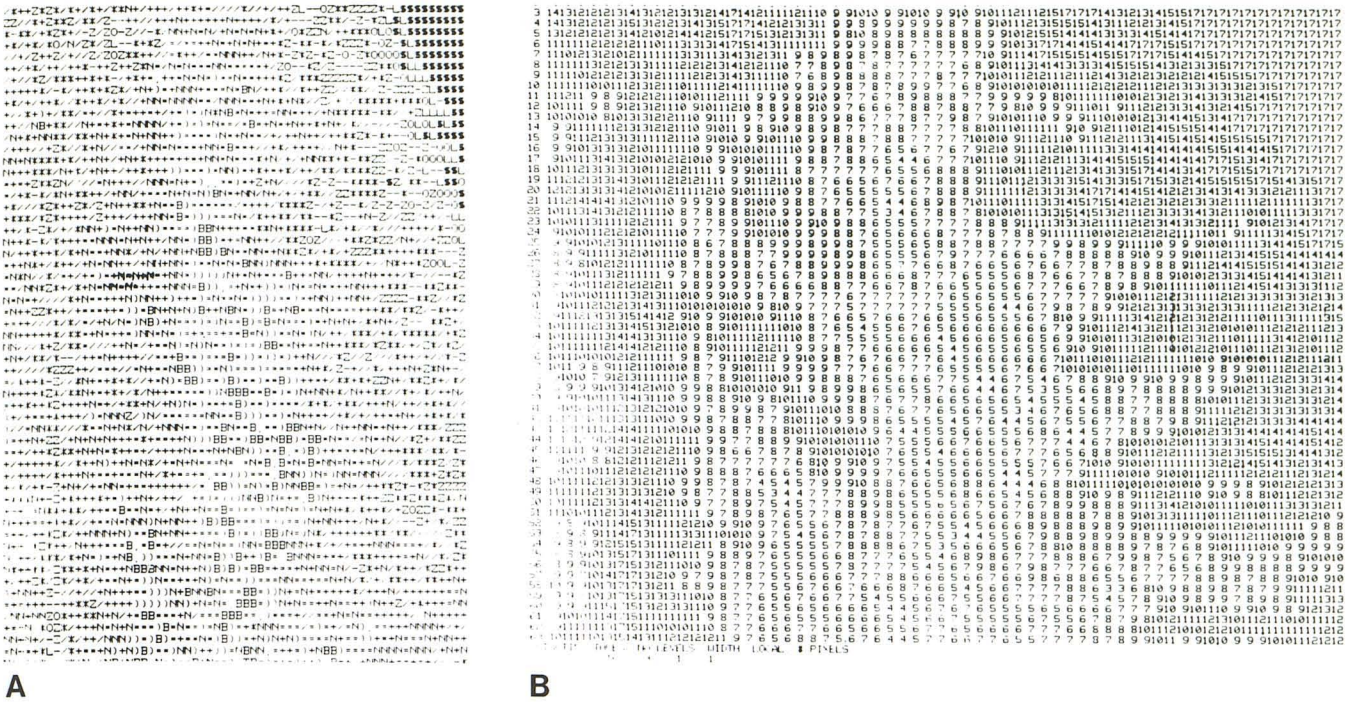

A B

Fig. 6.—**A**, Raw data of zoomed view of right upper quadrant of fig. 3A. Note wide variation of CT numbers (each symbol represents different CT number). **B**, Regional clustering algorithm applied to this data. Gray and white matter now are clearly demarcated.

to distinguish gray and white matter. Other methods (e.g., the global maximum-likelihood method) are difficult to use because of the small size of the spatial regions that are clearly white or gray matter.

The development in this study of the regional-clustering algorithm (based on the measured textural properties of gray and white matter) is a first step in the use of higher-order statistics for scene segmentation. Its potential has already been validated by a specially constructed textural phantom. Current research in image scaling, image orientation, and alignment will allow direct correlation with pathologic sections.

Finally, neonatal CT scans were used in this study as a standard for the evaluation of developing brain, while adult CT scans were used as the standard for evaluating abnormalities of myelinated mature brain. The results of our analysis showed no significant differences in the gray/white matter differentiation, even though the degree of myelination and water content of the white matter differed greatly between the two groups.

REFERENCES

1. Brooks RA, Di Chiro G, Keller MR. Explanation of cerebral white-gray contrast in computed tomography. *J Comput Assist Tomogr* **1980**;4:489–492
2. Dobbing J, Sands J. Quantitative growth and development of human brain. *Arch Dis Child* **1979**;48:757–769
3. Cahill PT, Knowles RJR, Kneeland B, Lee BCP. Segmentation of white/gray matter by a texture based clustering algorithm. In: *Proceedings of the 6th international conference on pattern recognition.* Silver Spring, MD: IEEE Computer Society, **1982**:633–636
4. Hanson KM. Detectability in computer tomographic images. *Med Phys* **1979**;6:441–445
5. Cahill PT, Knowles RJR, Tsen O, Pouapinya R. Evaluation of edge detection algorithms for nuclear medicine via roc and shape analysis with adaptive thresholding. *Proc Inst Electrical Electronic Eng* **1981**;28:64–68